Available online at www.eccomasproceedia.org
Eccomas Proceedia SMART (2023) 83-94

ECCOMAS
Proceedia

X ECCOMAS Thematic Conference on Smart Structures and Materials
SMART 2023
D.A. Saravanos, A. Benjeddou, N. Chrysochoidis and T. Theodosiou (Eds)

NUMERICAL INVESTIGATION ON THE RELATIONSHIP BETWEEN THE ACOUSTOELASTIC EFFECT AND THE MODAL PROPERTIES OF LAMB WAVES IN ALUMINUM

NATALIE RAUTER[*1], TILMANN BARTH[*2] AND ROLF LAMMERING[*3]

[*]Institute of Mechanics
Helmut Schmidt University / University of the Federal Armed Forces Hamburg
Holstenhofweg 85, 22043 Hamburg, Germany
e-mail: [1] natalie.rauter@hsu-hh.de, [2] barth@hsu-hh.de, [3] rl@hsu-hh.de
web page: http://www.hsu-hh.de/mechanik

Abstract. An in-service monitoring of structures with guided ultrasonic waves like Lamb waves always includes an interaction of the wave with a certain internal stress state. The interaction leads to a change of the phase velocity and hence, the propagation properties. To investigate the driving influences with respect to the numerical modeling in more detail a modal analysis is utilized to derive the displacement field components and the participation factors for a pre-stressed aluminum wave guide over a frequency range of up to $4\,\mathrm{MHz\,mm}$. Subsequently, both quantities are combined. Finally, the obtained curves for $\Gamma_j \hat{u}_i$ are compared with the course of the phase velocity change due to a pre-stress state of $10\,\mathrm{MPa}$ derived by the Neo-Hookean and Murnaghan material models. The comparison reveals a correlation between the relative displacement component in combination with the modal participation factor in the direction of the wave propagation on the one hand side and the behavior of the phase velocity under uniaxial tensile load on the other side. It appears that the out-of-plane component is predominant for the Murnaghan material model, whereas the Neo-Hookean material model ensures a more balanced representation of both in- and out-of-plane component.

Key words: Acoustoelastic Effect, Lamb Waves, Modal Analysis

1 INTRODUCTION

Guided ultrasonic waves are widely used in the fields of damage detection and structural health monitoring [1, 2, 3]. When applying guided ultrasonic wave based structural health monitoring in service the wave propagation takes place at different internal stress states, which lead to a change in the phase velocity [4, 5, 6]. This is also known as the acoustoelastic effect. Hence, to ensure an accurate interpretation of sensor data from health monitoring systems, knowledge about the influence of the internal stress states on the wave propagation is essential. There are still many open questions regarding the correct modeling approach to incorporate the acoustoelastic effect into numerical simulations.

© 2023 The Authors. Published by Eccomas Proceedia.
Peer-review under responsibility of the organizing committee of SMART 2023.
doi: 10.7712/150123.9767.444077

In the field of acousto-elasticity, early work was done by Biot [7, 8] who developed a theory of elastic waves under the effect of initial stress for geophysical systems. In the following, Hughes and Kelly [9], Thurston and Brugger [10] and Toupin and Bernstein [11] dealt with the determination of the third-order elastic constants via experiments for use in the constitutive theory of Murnaghan [12]. Early application for the determination of elastic stress states in bodies using longitudinal and or shear waves can be found among others in the work of Crecraft [13], Hsu [14], and Blinka and Sachse [15]. In Pao and Gamer [6] the theory of acoustoelasticity and also acoustoplasticity are reviewed with a focus on hyperelastic anisotropic materials and stress measurements via shear wave birefringence. Focusing on the material models used, reference should be made to the work of Man et al. [16] and Shams et al. [17] and references therein, which discuss the suitability of constitutive theories to represent pre- and residual stresses.

In the field of acoustoelastic Lamb waves theoretical approaches can be found in the work of Husson [18] and Qu and Liu [4], which deal with the influence of pre- and residual stresses on the wave propagation. Numerical investigations on this topic using the semi-analytical finite element method are presented, for example, in Wilcox [19], Loveday [20], and Yang [21]. There are not many experimental studies on this topic but Gandhi et. al. [22] investigate the acoustoelastic effect by measuring wave velocities of Lamb waves in biaxially stressed plates and compare the results with analytical results. Qiu et al. [23] investigate this relationship for uniaxially stressed plates and compare the results to numerical simulations with emphasis of multiphysical simulations regarding the piezoelectric transducers. In the work of Barth et al. [24] this relationship is investigated for uniaxially stressed plates and compared with numerical results. Here the emphasis is on investigating the effect over a large frequency range and with different hyperelastic material models.

It is shown, that well-known hyperelastic material models like the Neo-Hookean show a good agreement with experimentally obtained data [24]. However, the results differ significantly from the established modeling approach utilizing third-order elastic constants and therefore, the material model by Murnaghan [12]. To get a deeper understanding of the corresponding mechanisms the displacement field of the fundamental modes as well as the excited rigid body modes are analyzed.

It is suggested, that the influence of pre-stresses on the wave propagation might be linked to the composition of the displacement field and the corresponding modal participation factor, which holds information about the contribution of a given mode on the response of a system.

Therefore, the presented work covers the analysis of the fundamental wave modes' displacement field components and their modal participation factors with respect to the wave propagation in a pre-stressed aluminum sheet. This is done by extracting the displacement field and modal participation factors components of the fundamental S_0 and A_0 wave modes from a modal analysis for a frequency-thickness range of up to $4\,\mathrm{MHz\,mm}$. The modal participation factors are then combined with information about the relative in- and out-of-plane displacement field components of the fundamental wave modes.

Subsequently, the structure of the presented work is as follows. Section 2 holds a brief summary of the measurements regarding the acoustoelastic effect in an aluminum plate. Next

is the modal analysis in Section 3, which provides the determination of the displacement field components and the participation factors. Furthermore, the correlation between this quantities and the acoustoelastic effect is discussed. Finally, the work is concluded in Section 4.

2 ACOUSTOELASTIC EFFECT

2.1 Theoretical background

The acoustoelastic effect deals with the influence of static stress states on the wave propagation. To include this effect into numerical simulations the use of nonlinear material models is required. In context of guided ultrasonic waves in general and Lamb waves in particular this is done by incorporating the hyperelastic material model of Murnaghan [12], which uses so called third-order elastic constants to represent the nonlinear material behavior. With respect to isotropic material these are the parameters $l, m,$ and n, which lead to a total of 5 independent material parameters. The corresponding strain-energy density function reads

$$\Psi_{\text{Mur}}(\mathbf{E}) = \frac{1}{2}(\lambda + 2\mu)\left[\operatorname{tr}(\mathbf{E})\right]^2$$
$$-2\mu \operatorname{tr}(\mathbf{E}^2) + \frac{1}{3}(l + 2m)\left[\operatorname{tr}(\mathbf{E})\right]^3 - 2m \operatorname{tr}(\mathbf{E}) \operatorname{tr}(\mathbf{E}^2) + n \operatorname{tr}(\mathbf{E}^3), \tag{1}$$

where $\mathbf{E}$ is the Green-Lagrangian strain tensor and μ and λ are the Lamé-coefficients. However, the third-order elastic constants are difficult to determine and the procedure shows high uncertainties. Values can be found in [25]. To overcome this issue it is beneficial to use other well-known material formulation like the Neo-Hookean material models, which is given as a function of the right Cauchy-Green tensor $\mathbf{C}$ by [26]

$$\Psi_{\text{Neo}}(\mathbf{C}) = \frac{1}{2}\lambda\left[\ln(J)\right]^2 - \mu \ln(J) + \frac{1}{2}\mu\left[\operatorname{tr}(\mathbf{C}) - 3\right]. \tag{2}$$

The formulation of this hyperelastic material is much simpler than the formulation of the Murnaghan model and does not require any additional material parameters.

2.2 Numerical modeling

As done in [27, 28, 29] a linear modal analysis can be used to derive fundamental wave propagation properties numerically for large frequency ranges. This covers the frequency dependent phase velocity and hence, the dispersion diagrams as well as the corresponding displacement fields. As shown in [19, 20, 21, 24] this approach is not limited to unloaded wave guides but can also be used to derive dispersion curves for pre-stressed specimens.

Here, the investigations are based on a two-dimensional model representing a $0.1\,\mathrm{mm}$ wide part of the cross-section of an exemplary plate-shaped waveguide with a thickness of $1\,\mathrm{mm}$, see Figure 1 (a). A two-stage model is used to calculate the propagation properties of Lamb waves under pre-stress. In a first step, the pre-stress is applied by a nonlinear static analysis, the model of which is shown in Figure 1 (b). The results of this analysis are then transferred into a linear modal analysis, which is used to calculate the propagation properties of the Lamb

waves under pre-stress. Following the conditions for the propagation of Lamb waves in thin-walled structures the top and bottom edges have stress-free boundary conditions while on the right and left edge of the cross-section periodic boundary conditions are applied, marked blue in Figure 1 (c). For discretization second-order Lagrange elements are used.

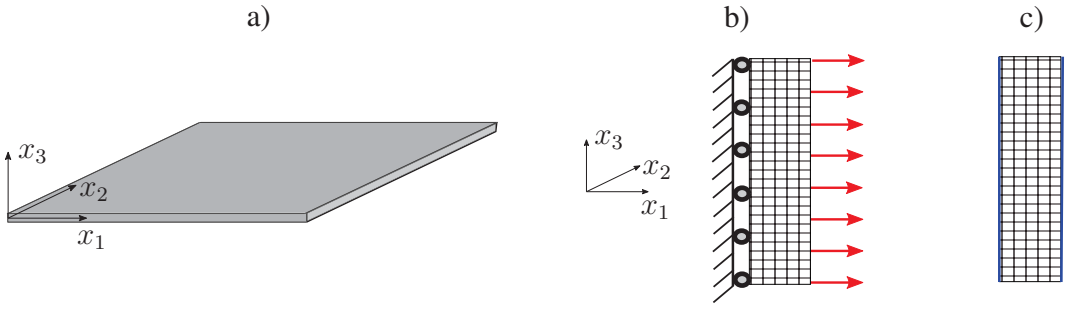

Figure 1: a) exemplary plate-shaped waveguide, b) finite element model for the static analysis, c) finite element model for the modal analysis, periodic boundary conditions marked in blue.

The corresponding material parameters for the linear and nonlinear domain of aluminum as well as the simulation specifications are summarized in Tables 1a and 1b.

Parameter	Value	Unit
length	0.1	mm
thickness	1	mm
Poisson's ratio	0.33	-
Density	2700	$\mathrm{kg\,m^{-3}}$
Young's modulus	68	GPa

(a) Specimen specification made from EN AW-5754.

Parameter	Value	Unit
l	-252.2	GPa
m	-325.0	GPa
n	-351.2	GPa

(b) Third-order elastic constants for EN AW-7075 [25].

Table 1: Model parameters.

2.3 Results

This model was used in previous work to simulate the effect of pre-stresses on the wave propagation properties. The resulting dispersion curves for the wave propagation in a pre-stressed aluminum plate are depicted in Figure 2 for the Murnaghan and Neo-Hookean material model. Additionally the results for a pure linear numerical simulation are indicated. Figure 2 (a) gives the change of the phase velocity for the a frequency-thickness range of up to $4\,\mathrm{MHz\,mm}$ for the S_0 wave mode, where as the corresponding curves for the A_0 wave mode are plotted in Figures 2 (b) and (c). The diagrams reveals the differences regarding the nonlinear modeling approach utilizing different hyperelastic strain energy density functions.

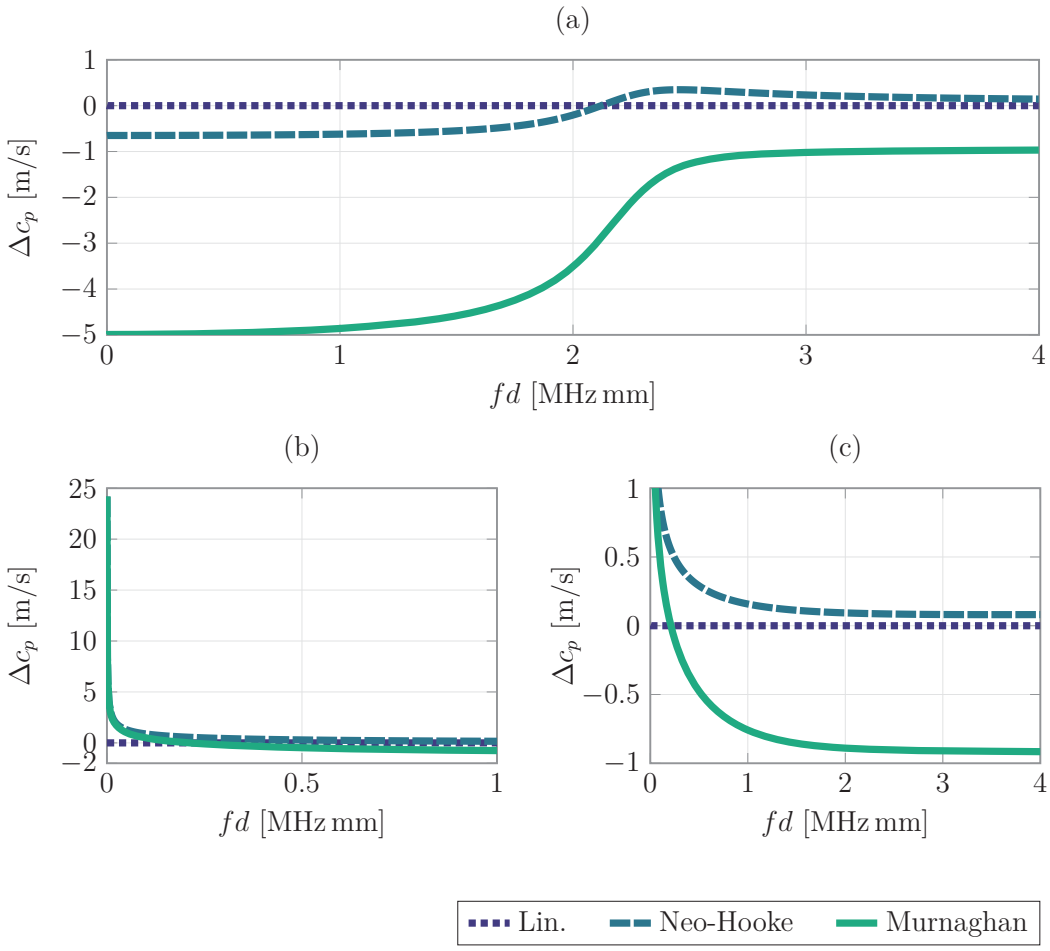

Figure 2: Change of phase velocity due to a prestress of 10 MPa for the fundamental S_0 (a) and A_0 (b and c) wave modes.

3 MODAL ANALYSIS

This section deals with the analysis of the displacement field and the modal participation factors to gain knowledge about the dominant displacement field component and its meaning regarding the influence of pre-stress on the wave propagation. The displacement field and participation factors are extracted from the same numerical model as used before for the dispersion relation. However, only linear elastic material behavior is considered.

3.1 Displacement field

In Figure 3 the displacement fields across the thickness of the fundamental S_0 and A_0 wave modes at a frequency thickness pair of 100 kHz mm are depicted. The results meet the expectation regarding axis and point symmetry [2, 3]. To derive the dominant displacement field

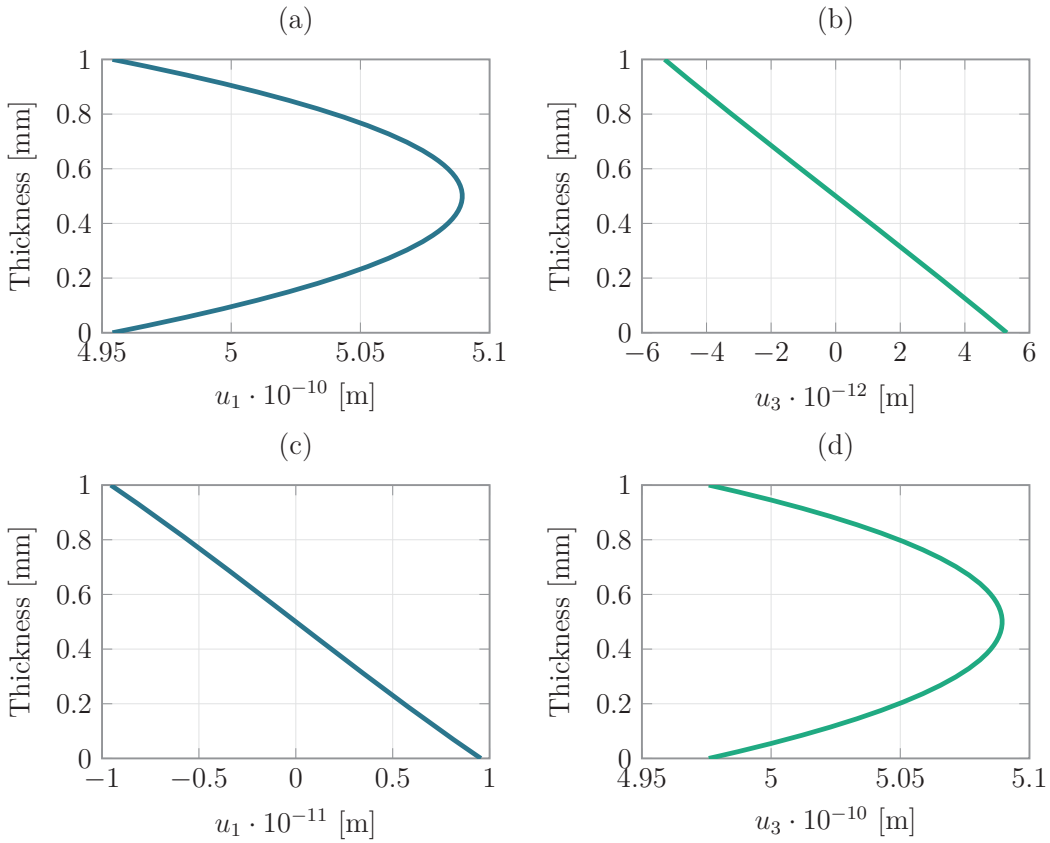

Figure 3: Displacement field components of Lamb waves in an aluminum plate at $100\,\mathrm{kHz\,mm}$. (a) and (b) the fundamental S_0 wave mode, (c) and (d) A_0 wave mode.

component and to analyze its behavior over a certain frequency range the relative amplitude is computed for the frequency thickness range of up to $4\,\mathrm{MHz\,mm}$. Taking into account the results for the displacement components at each node along the edge the relative amplitude is given by

$$\hat{u}_i = \sum_{k=1}^{N} \frac{|u_{ki}|}{\sqrt{u_{k1}^2 + u_{k3}^2}}, \tag{3}$$

where N is the number of nodes along the edge. The corresponding results are shown in Figure 4. The diagrams reveal that for the S_0 wave mode the in-plane component is dominant until a frequency thickness pair of approximately $2.5\,\mathrm{MHz\,mm}$. Beyond that, the out-of-plane component is dominant. For the A_0 wave mode the out-of-plane component is dominant over the whole frequency range. This meets the literature, where it is suggested to approximate the antisymmetric mode at low frequencies by a transverse wave [3].

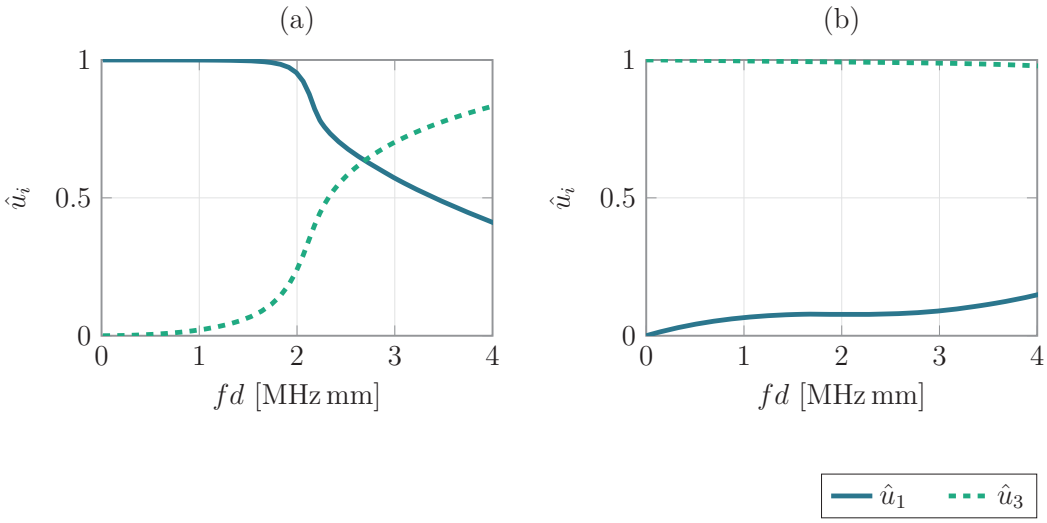

Figure 4: Relative amplitudes (a) of the S_0 and (b) of the A_0 mode for a frequency range of up to $4\,\mathrm{MHz\,mm}$.

3.2 Modal participation factors

The modal participation factor is a scalar value that indicates the measure of interaction between an eigenmode and a vector of unit displacement in the j-direction

$$\Gamma_j = \frac{\left[\mathbf{u}^T\right]\left[\mathbf{M}\right]\left[\mathbf{r}_j\right]}{\left[\mathbf{u}^T\right]\left[\mathbf{M}\right]\left[\mathbf{u}\right]}\,. \tag{4}$$

Here, the matrix $\mathbf{u}$ gives the eigenmode and the column matrix $\mathbf{r}_j$ contains the unit displacement in the j-direction. Finally, $\mathbf{M}$ gives the mass matrix. Since the modal participation factors are proportional to the reaction force of the rigid body motion, they indicate which mass fraction is involved in the corresponding eigenform Ist der Satz so ok?. The results for the modal participation factors with respect to the S_0 and A_0 wave modes are plotted in Figure 5 separately for the coordinate direction x_1 and x_3. Furthermore, the values are given with respect to the highest value for each mode.

The diagrams reveal that the S_0 wave mode is mostly driven by an in-plane rigid body motion. In contrast to this the out-of-plane component is neglectable. For the A_0 wave mode the opposite holds. Here, the in-plane component does not significantly contribute to the displacement of the eigenforms. Instead, the out-of-plane rigid body motion is considerably excited. Moreover, the decrease of the modal participation factor Γ_1 of the S_0 wave mode is more prominent than the decrease of Γ_3 of the A_0 wave mode. This correlates with the behavior of the relative amplitude presented in Figure 4.

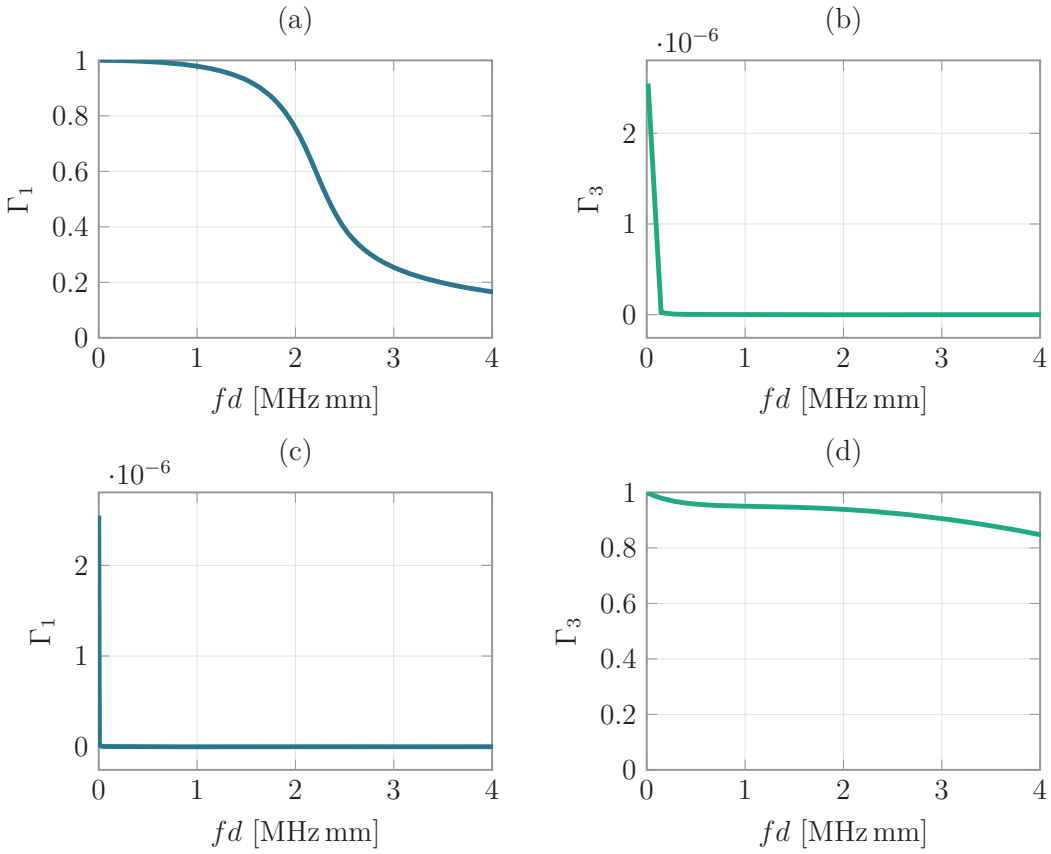

Figure 5: Modal participation factors of the fundamental wave modes in aluminum. (a) and (b) based on the S_0 wave mode with respect to x_1 and x_3, respectively. (c) and (d) based on the A_0 wave mode with respect to x_1 and x_3, respectively.

3.3 Sensitivity analysis

It is suggested that both the dominant displacement component and the involved mass during the wave propagation contribute to the acoustoelastic effect. Therefore, these two quantities are combined by computing the product

$$\Gamma_j \hat{u}_i. \tag{5}$$

The corresponding results with respect to x_1 are provided in Figure 6 for the fundamental S_0 and A_0 wave modes, respectively. In all figures the product $\Gamma_j \hat{u}_1$ is plotted with a negative sign to indicate the influence of pre-stress in x_1-direction on an in-plane displacement. From fundamental studies it is known that an external load in x_1-direction leads to a velocity reduction by a pure in-plane motion. The opposite holds for an out-of-plane motion. In this case, the velocity increases.

First of all in this work the wave propagation in x_1-direction is analyzed. This also em-

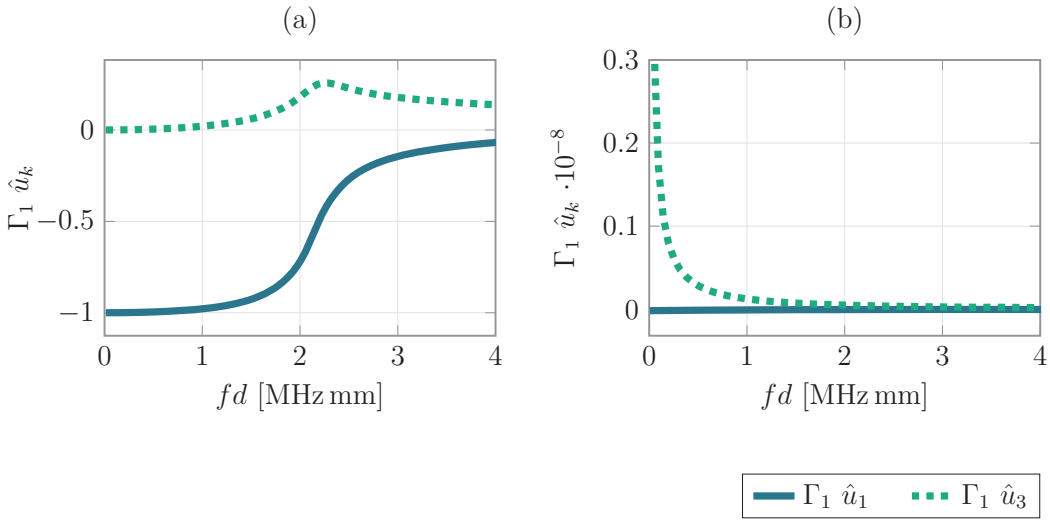

Figure 6: Product of the modal participation factor with the relative displacement field components of the fundamental S_0 and A_0 wave modes both with respect to x_1. (a) S_0 (b) A_0.

phasizes, that there is an energy flux in the direction that coincides with the wave propagation direction. Therefore, the analysis concentrates on the participation factor component in x_1-direction. Concerning this, Figure 6 (a) gives the product of Γ_1 with the relative displacement field components $\hat{u}_1$ and $\hat{u}_3$ for the S_0 wave mode. The same information is provided in Figure 6 (b) for the A_0 wave mode.

Starting with the fundamental S_0, Figure 2 (a) shows that for both material models first a decrease in the phase velocity due to a pre-stress state is observed. This corresponds very well to Figure 6 (a). At low frequencies the in-plane component is dominant and hence, induces a decreased phase velocity. With an increasing frequency the influence of the in-plane component $\Gamma_1\hat{u}_1$ decreases significantly and the out-of-plane component $\Gamma_1\hat{u}_3$ gets more important. Within the definition of the nonlinearity of the used material model these two effects are superimposed. A comparison with the results provided in Section 2 suggests that the material model by Murnaghan emphasis on the nonlinearity within the out-of-plane component where as the Neo-Hookean material model shows a more balanced influence of both components, indicated by the change in sign at approximately $2.1\,\mathrm{MHz\,mm}$. Transferring this on the results for the fundamental A_0 wave mode in Figure 6 (b) allows the same conclusion. Here, at first the out-of-plane component $\Gamma_1\hat{u}_3$ is dominant leading to an increased phase velocity. However, the influence of the out-of-plane decreases with an increasing frequency. At the same time the $\Gamma_{i1}\hat{u}_1$ is not equal to zero but very small. This means, that the in-plane component also contributes to the acoustoelastic effect at higher frequencies. Combining this with the results in Figure 2 (c) again indicates that the Murnaghan material modeling approaches might overestimate the nonlinear influence on the out-of-plane component leading to a change in sign, whereas the Neo-Hookean material modeling shows a more balanced behavior and therefore, a decrease of

the phase velocity is not predicted within this simulations. This also meets the results of experimental investigations and numerical simulations including only geometrical nonlinearities.

4 CONCLUSION

In this work the analysis of influencing factors for the acoustoelastic effect are presented. Therefore, the displacement fields and the participation factors are determined by utilizing a modal analysis. Combining the information with respect to the relative displacement component and the excited rigid body motions leads to a correlation with the change of the phase velocity due to an external loading. As known for fundamental one-dimensional oscillations an in-plane external loading causes a decreasing wave velocity for an in-plane motion and an increasing wave velocity for an out-of-plane motion. The same can be found here. However, it appears that the nonlinearity of the different material properties contributes differently to the in- and out-of-plane motion. Here, the Murnaghan material model seems to concentrate the nonlinear effect on the out-of-plane component, which promotes a decreasing phase velocity in comparison to the Neo-Hookean material model.

REFERENCES

[1] R. Lammering, Lamb-Wave Based Structural Health Monitoring in Polymer Composites, ser. Research Topics in Aerospace Ser. Cham: Springer International Publishing, 2017. [Online]. Available: https://ebookcentral.proquest.com/lib/kxp/detail.action?docID=4987978

[2] V. Giurgiutiu, Structural Health Monitoring: With Piezoelectric Wafer Active Sensors, 1st ed. s.l.: Elsevier professional, 2007. [Online]. Available: http://gbv.eblib.com/patron/FullRecord.aspx?p=330089

[3] J. L. Rose, Ultrasonic Guided Waves in Solid Media. Cambridge University Press, 2014.

[4] J. Qu and G. Liu, Effects of Residual Stress on Guided Waves in Layered Media. Boston, MA: Springer US, 1998, pp. 1635–1642. [Online]. Available: https://doi.org/10.1007/978-1-4615-5339-7_212

[5] Y. Pao, "Acoustoelasticity and ultrasonic measurement of residual stress," Physical Acoustics, pp. 61–143, 1984.

[6] Y. Pao and U. Gamer, "Acoustoelastic waves in orthotropic media," The Journal of the Acoustical Society of America, vol. 77, no. 3, pp. 806–812, 1985. [Online]. Available: https://doi.org/10.1121/1.392384

[7] M. A. Biot, "Non-linear theory of elasticity and the linearized case for a body under initial stress," The London, Edinburgh, and Dublin Philosophical Magazine and Journal of Science, vol. 27, no. 183, pp. 468–489, 1939.

[8] ——, "The influence of initial stress on elastic waves," Journal of Applied Physics, vol. 11, no. 8, pp. 522–530, 1940.

[9] D. S. Hughes and J. L. Kelly, "Second-order elastic deformation of solids," Physical Review, vol. 92, no. 5, pp. 1145–1149, 1953.

[10] R. N. Thurston and K. Brugger, "Third-order elastic constants and the velocity of small amplitude elastic waves in homogeneously stressed media," Phys. Rev., vol. 133, pp. A1604–A1610, Mar 1964. [Online]. Available: https://link.aps.org/doi/10.1103/PhysRev.133.A1604

[11] R. A. Toupin and B. E. Bernstein, "Sound waves in deformed perfectly elastic materials. acoustoelastic effect," Journal of the Acoustical Society of America, vol. 33, pp. 216–225, 1961.

[12] F. D. Murnaghan, Finite deformation of an elastic solid. NY: Dover Publications, 1951.

[13] D. Crecraft, "The measurement of applied and residual stresses in metals using ultrasonic waves," Journal of Sound and Vibration, vol. 5, no. 1, pp. 173–192, 1967. [Online]. Available: https://www.sciencedirect.com/science/article/pii/0022460X67901861

[14] N. N. Hsu, "Acoustical birefringence and the use of ultrasonic waves for experimental stress analysis," Experimental Mechanics, vol. 14, pp. 169–176, 1974.

[15] J. Blinka and W. Sachse, "Application of ultrasonic-pulse-spectroscopy measurements to experimental stress analysis," Experimental Mechanics, vol. 16, pp. 448–453, 1976.

[16] C.-S. Man and W. Y. Lu, "Towards an acoustoelastic theory for measurement of residual stress," Journal of Elasticity, vol. 32, pp. 159–182, 02 1987.

[17] M. Shams, M. Destrade, and R. Ogden, "Initial stresses in elastic solids: Constitutive laws and acoustoelasticity," Wave Motion, vol. 48, no. 7, pp. 552–567, 2011. [Online]. Available: https://www.sciencedirect.com/science/article/pii/S0165212511000436

[18] D. Husson, "A perturbation theory for the acoustoelastic effect of surface waves," Journal of Applied Physics, vol. 57, no. 5, pp. 1562–1568, 1985. [Online]. Available: https://doi.org/10.1063/1.334471

[19] F. Chen and P. D. Wilcox, "The effect of load on guided wave propagation," Ultrasonics, vol. 47, pp. 111–122, 2007. [Online]. Available: https://www.sciencedirect.com/science/article/pii/S0041624X07000753

[20] P. Loveday, "Semi-analytical finite element analysis of elastic waveguides subjected to axial loads," Ultrasonics, vol. 49, pp. 298–300, 12 2008.

[21] Z. Yang, Z. Wu, J. Zhang, K. Liu, Y. Jiang, and K. Zhou, "Acoustoelastic guided wave propagation in axial stressed arbitrary cross-section," Smart Materials and Structures, vol. 28, p. 045013, 2019. [Online]. Available: https://doi.org/10.1088/1361-665x/aadb6e

[22] N. Gandhi, J. E. Michaels, and S. J. Lee, "Acoustoelastic lamb wave propagation in biaxially stressed plates," The Journal of the Acoustical Society of America, vol. 132, no. 3, pp. 1284–1293, 2012. [Online]. Available: https://doi.org/10.1121/1.4740491

[23] L. Qiu, X. Yan, X. Lin, and S. Yuan, "Multiphysics simulation method of lamb wave propagation with piezoelectric transducers under load condition," Chinese Journal of Aeronautics, vol. 32, 02 2019.

[24] T. Barth and R. Lammering, "Numerical investigations on the influence of prestress on lamb wave propagation," in European Workshop on Structural Health Monitoring, P. Rizzo and A. Milazzo, Eds. Cham: Springer International Publishing, 2023, pp. 3–12.

[25] D. Stobbe, "Acoustoelasticity in 7075-t651 aluminum and dependence of third order elastic constants on fatigue damage," Dissertation, Georgia Tech, 2005.

[26] T. Belytschko, W. Liu, B. Moran, and K. Elkhodary, Nonlinear Finite Elements for Continua and Structures. Wiley, 2013.

[27] J. M. Galán and R. Abascal, "Numerical simulation of lamb wave scattering in semi-infinite plates," International Journal for Numerical Methods in Engineering, vol. 53, no. 5, pp. 1145–1173, 2002. [Online]. Available: https://onlinelibrary.wiley.com/doi/abs/10.1002/nme.331

[28] H. Gao, "Ultrasonic guided wave mechanics for composite material structural health monitoring," Dissertation, The Pennsylvania State University, 2007.

[29] Z. A. B. Ahmad, "Numerical simulations of lamb waves in plates using a semi-analytical finite element method," Dissertation, Otto von Guericke University, Magdeburg, 2011.